OPTICAL REVIEW Vol. 4, No. 1A (1997) 89-91

Blue Light-Emitting-Diode-Pumped Point Temperature Sensor Based on a Fluorescence Intensity Ratio in Pr^{3+}: ZBLAN Glass

Eric MAURICE,[1] Gerard MONNOM,[1] Greg W. BAXTER,[2] Scott A. WADE,[2] Bill P. PETRESKI[2] and Stephen F. COLLINS[2]

[1] *Laboratoire de Physique de la Matière Condensée-CNRS-UA 190, Université de Nice-Sophia Antipolis, 06108 Nice Cedex 2, France,* [2] *Optical Technology Research Laboratory—Department of Applied Physics, Victoria University, PO Box 14428 MCMC Melbourne, Victoria 8001, Australia*

(Received July 1, 1996; Accepted September 12, 1996)

A fluorescence intensity ratio technique has been applied to Pr^{3+}: ZBLAN glass, realising a point temperature sensor. We present data for a blue light emitting diode-pumped prototype which provides accurate and self-referenced measurements.

Key words: optical fiber, sensor, temperature, rare-earth, fluorescence, intensity ratio

1. Introduction

The fluorescence intensity ratio is a technique recently proposed[1,2] and investigated for point[3,4] and quasi-distributed[5] temperature sensors. This technique is based on the thermal coupling of two nearby energy levels of a rare earth ion. A system based on this effect requires a single optical source, which excites one of the desired levels; a Boltzmann distribution between the populations of the two coupled levels is then reached quasi-instantaneously. Ideally, the ratio of the populations of these two levels, and consequently the ratio of their fluorescence intensities, are independent of pump fluctuations, and hence are dependent on temperature alone. Therefore, this technique provides a self-referenced temperature measurement, which is important for the accurary and reliability of the sensor.

Previous work using the fluorescence intensity ratio of the green fluorescence of erbium doped silica fibre[6] demonstrated that a high power laser diode would be suitable for a practical device. However, in order to minimise cost, pump powers of a few milliwatt are desirable. An alternative may have been to enhance the green emission of the Er^{3+} ion by incorporating it in a low phonon energy host, such as fluorozirconate glass (ZBLAN). Unfortunately, in this glass, the non-radiative relaxation becomes predominant at elevated temperatures, so that the total Er^{3+} green fluorescence intensity suffers a severe drop at temperatures above 150°C.[1] The purpose of the current work is to develop a sensor which is both pumped by an inexpensive source and operational up to the maximum useful temperature of ZBLAN (about 250°C).

The effect of thermalisation between the $^3P_0$ and ($^3P_1$+$^1I_6$) energy levels of the Pr^{3+} ion doped into ZBLAN is first illustrated for various temperatures between −60 and 220°C. A novel temperature sensor prototype, pumped by a blue LED (allowing direct pumping of the desired levels) is then investigated for sensor performance, realising an accuracy of better than 1°C across a 300°C temperature range (−45→255°C). Furthermore, it is shown that variations as large as one order of magnitude of the LED power affect the indicated temperature by less than 1°C.

2. Thermal Coupling of the $^3P_0$ and ($^3P_1$+$^1I_6$) Energy Levels of Pr^{3+}

The ratio, R, of the fluorescence intensities of two thermally coupled energy levels of a rare earth ion, labelled $^{2S+1}L_J$ and $^{2S'+1}L'_J$, and the sensitivity, S, of a sensor based on this effect can be expressed as follows:

$$R=\frac{\sigma'}{\sigma}\frac{(2J'+1)}{(2J+1)}e^{-\frac{\Delta E}{kT}} \tag{1}$$

$$S=\frac{1}{R}\frac{\partial R}{\partial T}=\frac{\Delta E}{kT^2} \tag{2}$$

where the prime refers to the higher energy level, σ represents the emission cross-section of the level and ($2J$+1) its degeneracy, ΔE is the energy gap between the two levels, k is Boltzmann's constant and T is the absolute temperature. A temperature device accurate to better than 1°C requires sensitivities near 1%/°C. Therefore, from equation (2), energy levels with a gap of several hundred cm^{-1} would be required for a sensor operating near 20°C. However, (assuming levels of similar degeneracy and emission cross section) the emission from the upper level will be a small fraction of that from the lower level. As a consequence, temperature measurements will become less accurate since the emission peak resulting from the higher energy level will be masked by the tail of the dominant lower energy peak. By selecting thermally coupled levels with very different degeneracies this effect may be overcome.

Fortunately, the degeneracy ratio of 1 : 16 for the $^3P_0$ and the ($^3P_1$+$^1I_6$) energy levels of the Pr^{3+} ion is large (the $^3P_1$ and $^1I_6$ levels are sufficiently close to be considered a single level). Relevant aspects of the energy scheme of the Pr^{3+} ion are shown in Fig. 1(a).

Figure 1(a) indicates that the Pr^{3+} ion can be excited in the blue across a relatively large spectral range (440 to 480 nm), which is due to the proximity of $^3P_0$, $^3P_1$, $^1I_6$ and $^3P_2$ levels. We have investigated fluorescence for the $^3P_0$→$^1G_4$ and ($^3P_1$+$^1I_6$) →$^1G_4$ infrared transitions, which are sufficiently far from the pump wavelength to be detected separately in a practical device. Figure 1(b) presents the evolution of fluorescence spectra of these transitions as the

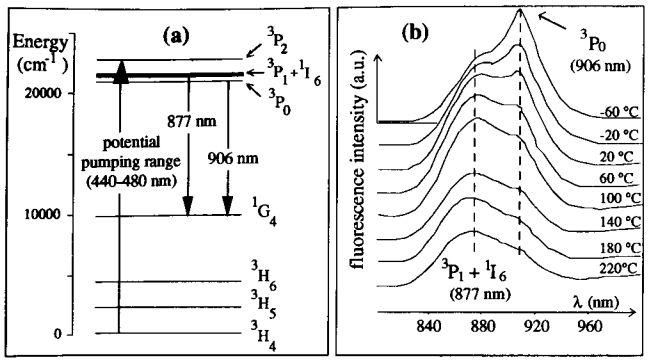

Fig. 1. (a) Simplified energy scheme of Pr^{3+} in ZBLAN. (b) Emission of the $^3P_0$ and $(^3P_1+^1I_6)$ levels at temperature ranging from −60°C to 220°C.

temperature is increased from −60°C to 220°C. Preliminary data were recorded using a 476 nm argon ion laser pump. The pump beam was launched into a 600 μm core diameter fibre whose other end was fixed to a 1% doped Pr^{3+} ZBLAN bulk sample. To maximise the stability of the arrangement, the sample was placed into a 500 gram-aluminium cylinder with its temperature monitored by a thermocouple placed in contact. The counter-propagating fluorescence was recorded using an optical spectrum analyzer (OSA). Figure 1(b) shows clearly that the ratio of the $(^3P_1+^1I_6)$ emission to the $^3P_0$ emission increases with temperature. The emission wavelengths of these levels appear to peak at 877 nm and 906 nm respectively, which implies an energy gap of 365 cm^{-1}. Using Eq. (2), this corresponds to a sensitivity of 0.58%/°C at 20°C. In addition, the spectra show that the combined fluorescence intensity does not drop significantly at high temperature, and that each of the $(^3P_1+^1I_6)$ and $^3P_0$ emissions can be identified across the entire investigated temperature range, as expected.

3. Blue LED-pumped Prototype

The blue LED had an optical power of 2 mW and a 60 nm full width at half-intensity-maximum emission spectrum centred at 450 nm (overlapping well with the blue absorption band of Pr^{3+}). Its beam was collimated (Fig. 2(a)) by the L1-lens through the M1-dichroic mirror, and focused into a 600 μm-core diameter silica-silicone fibre by the L2-microscope objective. The typical launched power was 100 μW. This guiding fibre was selected as it is tolerant of high temperatures, and matches well with the optogeometrical characteristics of the LED. The counter-propagating fluorescence guided by the fibre was collimated by L2 and reflected by M1. The $^3P_0$ and $(^3P_1+^1I_6)$ emissions were separated by the M2 and M3 filters and focused on the D1 and D2 detectors respectively. The spectral range analysed by each detector (Fig. 2(b)) was recorded with an OSA by launching a flat spectrum infrared source into the other end of the fibre. The peak wavelengths of the detectors (910 nm and 870 nm), were chosen to lie off the central wavelengths, as these evolve less rapidly with temperature. The LED was modulated at 270 Hz, and the signals from the detectors were monitored synchronously by two lock-in amplifiers, using a 3 second-time constant.

4. Sensor Performance

Figure 3(a) presents the temperature evolution of the R-ratio in the −45°C→255°C temperature range. The sensitivity of the sensor was measured to be 0.48%/°C at 20°C, which is close to the maximum sensitivity predicted, due to the good selectivity of the spectral ranges analysed by the detectors. For simplicity, a 3rd order polynomial has been fitted to the data. The accuracy of the sensor can be

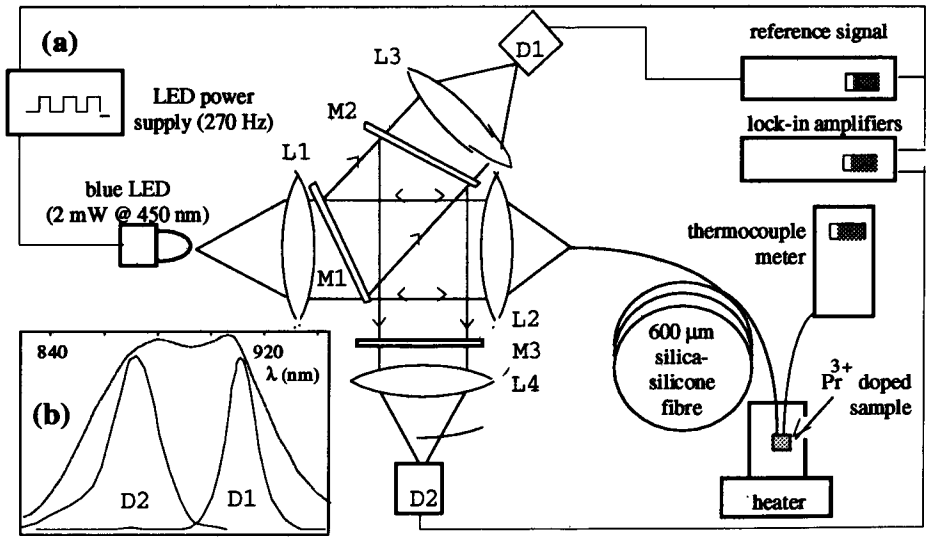

Fig. 2. (a) Temperature sensor prototype pumped by a blue LED. L1: lens (f=+25 mm). L2: ×20 microscope objective. L3, L4: lenses (f=+40 mm). M1: dichroic mirror (T=60% @450±30 nm, R=90% @900±50 nm). M2: dichroic-absorbent filter (T=80% @910 nm, T<1% @870 nm, T=0% @450 nm, R=85% @870 nm). M3: dichroic-absorbent filter (T=40% @870 nm, T<1% @910 nm, T=0% @450 nm). D1, D2: large area (5 mm^2) silicon detectors. (b) Spectral ranges analysed by the D1 and D2 detectors and Pr^{3+} emission spectrum at 20°C (dotted line). For clarity, the D1 and D2 curves have been normalised to the same value. The D2 curve was measured to be 2.4 times lower than the D1 curve.

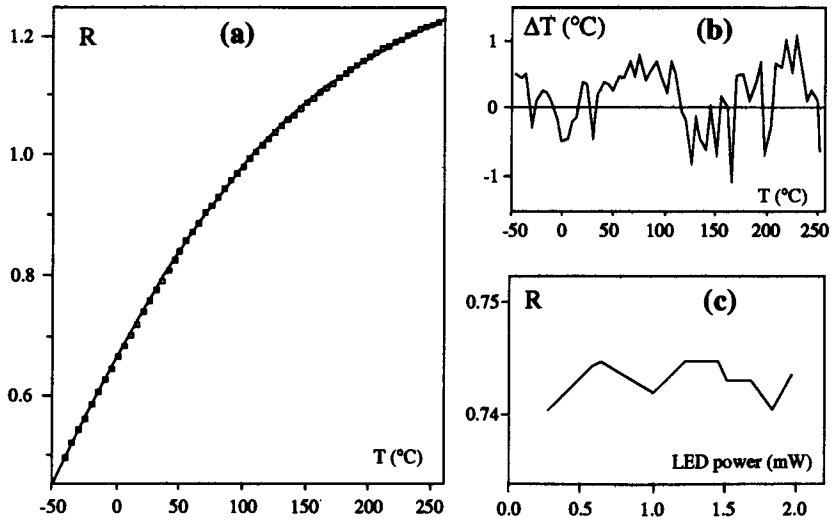

Fig. 3. (a) Variation of the R-ratio in the −45°C→255°C range. The continuous line is a 3rd order polynomial fit. (b) Temperature errors, determined as the difference between the measured data and the polynomial fit. (c) Evolution of the R-ratio, at constant temperature (20°C), versus the pump power.

determined as the difference, ΔT, between the measured ratio and the polynomial fit (Fig. 3(b)). The sensor demonstrates temperature errors less than 1°C across the investigated range, with a standard deviation of 0.4°C. In addition, Fig. 3(c) shows that the R-ratio at 20°C was changed by less than 0.4% when the pump power was varied by one order of magnitude, clearly demonstrating the advantages of a self-referenced measurement.

Figure 3(b) shows systematic deviations, which are reproducible from one experiment to another, and are consequences of the approximate nature of the 3rd order polynomial fit. This suggests that the accuracy of the sensor could be improved by the use of a more complex calibration curve.

The upper limit of the temperature range investigated was fixed by the thermal properties of the ZBLAN glass whilst the lower limit was set by the silica-silicone fiber. Indeed, the refractive index of silicone becomes higher than silica below −50°C, suppressing the guided wave effect. As can be seen in Fig. 1(b), the $(^3P_1+{}^1I_6)$ emission is still important at −60°C, suggesting that the measuring range of the sensor could be extended to much lower temperatures by choosing an appropriate guiding fiber.

In conclusion, we have demonstrated a fibre optic point temperature sensor pumped by an inexpensive source. The system investigated had an accuracy better than 1°C across a 300°C temperature range.

Acknowledgments

The authors wish to thank the members of the Photonics Section, at Telstra Research Laboratories, for access to rare-each-doped glass samples. S.A. Wade would like to acknowledge the financial support of the Australian Government through the provision of an Australian Postgraduate Award (APA) scholarship.

References

1) H. Berthou and C.K. Jorgensen: Opt. Lett. **15** (1990) 1100.
2) E. Maurice, G. Monnom, B. Dussardier, A. Saïssy, D.B. Ostrowsky and G.W. Baxter: Opt. Lett. **19** (1994) 990.
3) E. Maurice, G. Monnom, D.B. Ostrowsky and G.W. Baxter: Proc. SPIE **2360** (1994) 219.
4) E. Maurice, G. Monnom, D.B. Ostrowsky and G.W. Baxter: J. Lightwave Technol. **7** (1995) 1349.
5) E. Maurice, G. Monnom, D.B. Ostrowsky and G.W. Baxter: Appl. Opt. **34** (1995) 4196.
6) E. Maurice, G. Monnom, B. Dussardier, A. Saïssy, D.B. Ostrowsky and G.W. Baxter: Appl. Opt. **34** (1995) 8019.